JPE 16-3-29

http://dx.doi.org/10.6113/JPE.2016.16.3.1122
ISSN(Print): 1598-2092 / ISSN(Online): 2093-4718

A Sliding Mode Control Design based on the Reaching Law for Matrix Rectifiers

Zhiping Wang[*,**,***], Yunshou Mao[*], Zhanhu Hu[†], and Yunxiang Xie[***]

[*]School of Automation, Guangdong University of Technology, Guangzhou, China
[†,**]Guangdong Institute of Automation, Guangzhou, China
[***]School of Electric Power, South China University of Technology, Guangzhou, China

Abstract

This paper presents a novel approach for achieving both a tight DC voltage regulation and a power factor control by applying the Reaching Law Sliding Mode Control (RL-SMC) and the conventional Sliding Mode Control (SMC). Applying these strategies on a matrix rectifier (MR) can achieve a unity grid side power factor when the DC load changes widely and it can provide a ripple-free output voltage that is easily affected by distortions of the three-phase ac voltage supply. Furthermore, by employing the reaching law on the SMC can solve the chatting problem of the sliding motion. Comparative Matlab simulations and experimental verifications for these strategies have been presented and discussed in this paper. The results show that by applying the SMC and RL-SMC on a MR can achieve a unity grid side power factor and a regulated ripple-free DC output.

Key words: Input power factor, Matrix rectifier, Reaching law, Sliding mode control

I. INTRODUCTION

The conventional rectification, uncontrolled rectifiers and phase controlled rectifiers, may bring about a large number of harmonics, which have become the main 'pollution' of the grid. In addition, such 'pollution' makes other electric devices work improperly. Matrix Converters (MC) can be traced to the late 1970s [1]. The three phase to two phase AC-DC MC, i.e. matrix rectifier, can be deduced from the conventional three phase to three phase MC. The MR has several advantages: (1) operation in all four quadrants; (2) no need for a large value DC capacitor on the output side; (3) easy safe current commutation; (4) intrinsic buck converter and (5) power factor regulation [2]-[3]. Because of the advantages mentioned above, the MR has become a strong candidate for potential applications in plug-in automotive, aircraft, DC motor drives, etc. [4]. Moreover, the MR is the first stage of a two-stage matrix converter, and it can be used in the field of wind power generation and has wide application prospects and potential economic value.

Commonly there are several modulation algorithms for the MR, and they are the Alesina–Venturini optimum (A-V optimum) method [5], the Roy method [6] and the Space Vector Modulation (SVM) [7]. However, these algorithms are open-loop control. When applying these modulation algorithms on a MR, the performance of the DC output voltage becomes bad, since such modulation algorithms cannot resist disturbances.

An input filter is necessary for a sinusoidal input current because it can filter the harmonic components of the input current. However, the input filter's characteristics make the input power factor (IPF) remain high in the presence of high output loads, and the IPF degrades significantly under light-load conditions [8]. What is more, due to the presence of a grid side unbalanced input voltage and voltage disturbances, a MR cannot provide a ripple-free DC output voltage, and periodic oscillations appear.

In order to mitigate the fluctuations of the DC output voltage cause by the grid side unbalanced input voltage and to improve the IPF, scholars have carried out a lot of research in these fields. In [9], the static and power characteristics of

Manuscript received Jun. 24, 2015; accepted Jan. 26, 2016
Recommended for publication by Associate Editor Sangshin Kwak.
[†]Corresponding Author: 20140956@qq.com
Tel: +86-20-87682474, Guangdong Institute of Automation
[*]School of Automation, Guangdong University of Technology, China
[**]Guangdong Institute of Automation, China
[***]School of Electric Power, South China Univ. of Technology, China

the MR have been given. This has been a crucial support in terms of further research on control strategies. In [10], the designs of a feedforward control strategy was proposed to guarantee the stability of the DC output voltages. In [11], the designs of an opened-loop control, and in [12]-[13], the designs of closed-loop control strategies were proposed to compensate the power factor. As a result, applying feedforward control strategies to improve the performance of DC output voltage regulation can restrain disturbances of the unbalanced three-phase input to a certain extent. However, the performance is not obvious. In [14], a new-direct SVM based on an API controller was shown, and its correctness and effectiveness had been verified. However, PI control is a linear control, and its dynamic properties is poor. In [15], in order to improve dynamic performance, the conventional SMC was applied to compensate the input power factor and the DC output. A PI controller and a SMC controller were employed separately in the prototype experiment. The experiment results reveal that the dynamic properties of the SMC are superior. However, the output ripple voltage and input current harmonics are much more serious than those regulated by a PI controller.

In this paper, a novel approach to achieve both a tight DC voltage and a grid side power factor is proposed. The DC output voltage is controlled by a RL-SMC and the grid side power factor is compensated by the conventional SMC. Simulation and experimental results show that the proposed algorithm can fulfill the presupposed goals and alleviate chattering of the sliding mode.

II. Mathematical Model of a PMSM for Back-EMF Estimation

A. Space Vector Modulation Method

Fig. 1 shows the topology of the MR and this topology consists of 6 parts: a three-phase power source, input damping filters, a main circuit with six bidirectional switches, an output filter, and a load.

Space vector modulation (SVM) is used to provide sinusoidal input currents for the MR. The SVM must satisfy the following two constrains simultaneously:

(1) The existence theorem of the matrix converter theories in [16]-[17].

(2) The maximization of the DC output voltage to achieve full use of the input line–line voltages.

To satisfy the above constrains, only nine feasible switching states of the six bidirectional switches exist, and these nine states determine nine vectors which can be divided into two categories: active vectors (I_1 - I_6) and zero vectors (I_7 - I_9) .

In addition, the space vector hexagon is divided into six sectors by the active vectors, as shown in Fig. 2. The reference

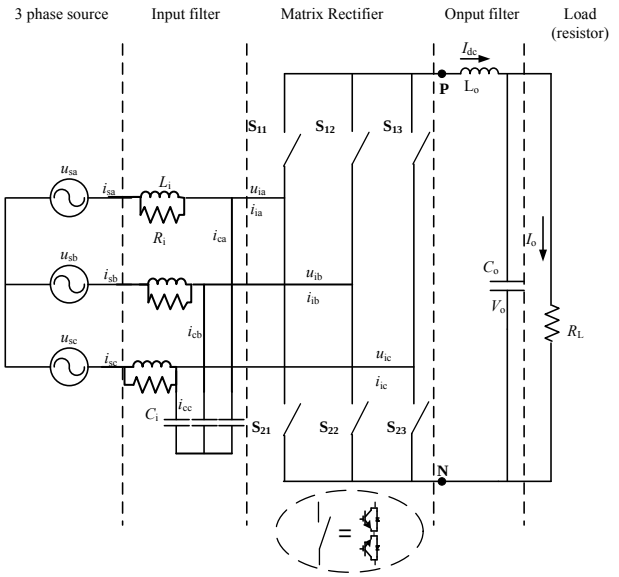

Fig. 1. Topology of the MR.

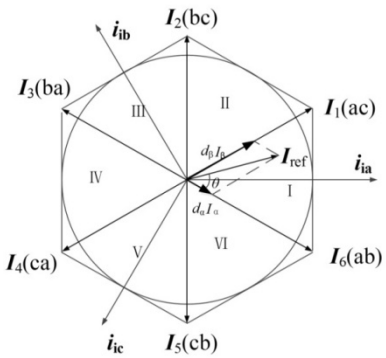

Fig. 2. Space vector diagram of input current.

current vector I_{ref} , synthesized from the two adjacent vectors I_α and I_β , and a zero vector, as shown in Fig. 3. θ is the angle between I_{ref} and its right adjacent active vector I_α , and $\theta \in [0, \pi/3]$. The reference current vector I_{ref} can be calculated as the following expression:

$$I_{\text{ref}} = \frac{T_\alpha(\theta)}{T_S} I_\alpha + \frac{T_\beta(\theta)}{T_S} I_\beta + \frac{T_0(\theta)}{T_S} I_0 \tag{1}$$

where $T_\alpha(\theta)$, $T_\beta(\theta)$ and $T_0(\theta)$ are the durative times of I_α , I_β and I_0 in one switching period T_S . The duty cycle $d_\alpha(\theta)$, $d_\beta(\theta)$ and $d_0(\theta)$ can be calculated as follows:

$$d_\alpha(\theta) = T_\alpha(\theta)/T_S = m\sin\left(\frac{\pi}{3} - \theta\right) \tag{2}$$

$$d_\beta(\theta) = T_\beta(\theta)/T_S = m\sin(\theta) \tag{3}$$

$$d_0(\theta) = 1 - d_\alpha(\theta) - d_\beta(\theta) \tag{4}$$

where m is the modulation index, $m \in [0,1]$. The averaged output voltage in a switching period can be calculated as:

$$V_{\text{PN}} = 1.5 m V_{\text{im}} \cos\varphi_{\text{i}} \tag{5}$$

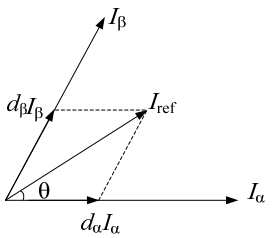

Fig. 3. Reference input-current space vector with the adjacent vectors.

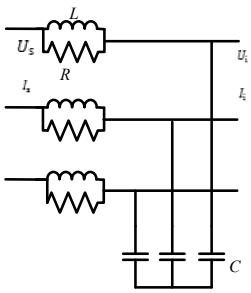

Fig. 4.The input filter of the MR.

where V_{im} is the amplitude of the input phase voltage, and φ_i is the desired input current displacement angle.

B. Input filter Analysis of the MR

The input filter, as shown in Fig. 4, is designed to filter the high harmonic components of the input current and to reduce the input voltage distortion supplied to the MR. In this topology, to damp the oscillations resulting from the matrix rectifier hard switching, the resistance is connected in parallel with the inductance, and this topology provides the minimization of power losses [18].

In the Fig. 4, U_s and I_s denote the input voltage and current at the grid side, and U_i and I_i denotes the input voltage and current of the MR. The IPF issue is addressed only when the input filter is considered. At the grid side, let $U_s = U_{sm}\angle\alpha$ and $I_s = I_{sm}\angle\beta$. At the output side of the filter, let $I_{in} = I_{im}\angle(\alpha-\varphi_i)$. To analyze Fig. 4, it should be known that:

$$j\omega CU_s + I_{in} = I_s\left(\frac{R^2+\omega^2L^2-\omega^3R^2LC}{R^2+\omega^2L^2} + j\frac{\omega^3L^2RC}{R^2+\omega^2L^2}\right) \quad (6)$$

It should be noted that $j\frac{\omega^3L^2RC}{R^2+\omega^2L^2}$ is so small that it can be ignored. Eq. (6) can be simplified as:

$$j\omega CU_{sm}\angle\alpha + I_{im}\angle(\alpha-\varphi_i) = \left(\frac{R^2+\omega^2L^2-\omega^3R^2LC}{R^2+\omega^2L^2}\right)I_{sm}\angle\beta \quad (7)$$

According to Eq. (7) and Fig. 5, the grid side power factor can be calculated as follows:

$$\varphi_s = \alpha-\beta = -\arctan\frac{\omega CU_{sm} - I_{im}\sin\varphi_i}{I_{im}\cos\varphi_i} \quad (8)$$

where α and β are the phase angles of the input voltage and input current at the grid side, respectively, φ_s is the grid side power factor angle, and φ_i is the switch matrix power factor angle. From Eq.(8), the phase shift φ_s is imposed by the MR's input filter, and the phase shift relates to the whole circuit including the DC loads.

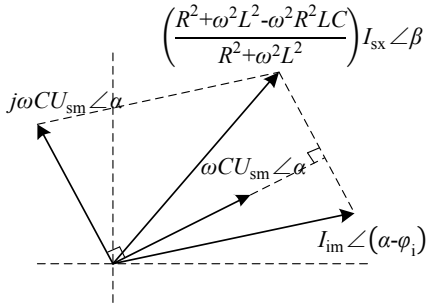

Fig. 5. Vector diagram of the Eq.(7).

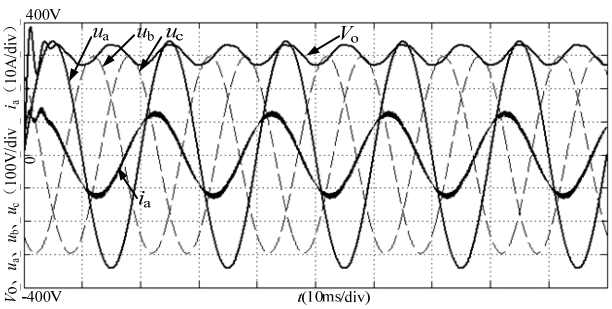

Fig. 6. Input and Output voltage waveform of the MR.

C. Impact of the DC Output Voltage Caused by an Imbalanced Input Voltage

According to the symmetrical components method, an unbalanced three-phase input voltage V_s can be decomposed into positive sequence component V_{sp} and negative sequence component V_{sn} as follows:

$$V_s = V_{sp} + V_{sn} = \begin{bmatrix} V_{PM}\cos(\omega t) \\ V_{PM}\cos(\omega t - \frac{2\pi}{3}) \\ V_{PM}\cos(\omega t + \frac{2\pi}{3}) \end{bmatrix} + \begin{bmatrix} V_{NM}\cos(\omega t) \\ V_{NM}\cos(\omega t + \frac{2\pi}{3}) \\ V_{NM}\cos(\omega t - \frac{2\pi}{3}) \end{bmatrix} \quad (9)$$

In Eq. (9), V_{PM} and V_{NM} denote the amplitudes of the positive and negative sequence input phase voltages, respectively, and ω is the input voltage angular frequency. Let the initial phase angles of the positive and negative sequence components become zero.

In [19]:

$$\psi_{ref} = m\begin{bmatrix} \cos(\omega t) \\ \cos(\omega t - \varphi_i - \frac{2\pi}{3}) \\ \cos(\omega t - \varphi_i + \frac{2\pi}{3}) \end{bmatrix} \quad (10)$$

Hence, the DC output voltage can be shown as:

$$V_{PN} = \psi_{ref}^T V_s = 1.5mV_{PM}\cos\varphi_i + 1.5mV_{NM}\cos(2\omega t + \varphi_i) \quad (11)$$

In Eq. (11), under the imbalanced three-phase voltage input condition, the output DC voltage of the Matrix Rectifier contain a ripple wave with a frequency that is double that of the input ripple wave except for the desired DC output voltage (as shown in Fig. 6).

III. SLIDING MODE CONTROL SYSTEM BASED ON THE REACHING LAW

The sliding mode control is one of the variable structure control strategies (VSC). The SMC has several advantages such as a quick response, strong robustness, and simple implementation. In addition, it is not affected by system parameter and external disturbances and it has good dynamic performance. However, the SMC makes the system switch between two kinds of states, which results in a tremendous chattering around the sliding surface when the system operates in the sliding mode. These problems have been tackled by using the Reaching Law on the SMC.

A. Mathematical Model of the System

After tangent calculus is applied to Eq. (8), it can be shown as:

$$\tan\varphi_s = -\frac{\omega C U_{sm}}{I_{im}\cos\varphi_i} + \tan\varphi_i \tag{12}$$

where φ_s is the grid side power factor angle. Assuming $\varphi_s < \pi/6$ and $\varphi_i < \pi/6$, the output power of the MR is shown as $P_{out} = \frac{V_o^2}{R_L} = 3U_{sm}I_{im}\cos\varphi_i$. Therefore, Eq. (8) can be shown as:

$$\varphi_s = -\frac{3\omega_i R_L C_i U_{sm}^2}{V_o^2} + \varphi_i \tag{13}$$

From Fig. 1, according to Kirchhoff's law, the following two equations are known:

$$\begin{cases} V_{PN} - V_o = L_o \dfrac{dI_{dc}}{dt} \\ I_{dc} - \dfrac{V_o}{R_L} = C_o \dfrac{dV_o}{dt} \end{cases} \tag{14}$$

Thus, the equation for the state of the output voltage and current can be given as:

$$\begin{bmatrix} \dot{V}_o \\ \dot{I}_{dc} \end{bmatrix} = \begin{bmatrix} -\dfrac{1}{R_L C_o} & \dfrac{1}{C_o} \\ -\dfrac{1}{L_o} & 0 \end{bmatrix} \begin{bmatrix} V_o \\ I_{dc} \end{bmatrix} + \begin{bmatrix} 0 \\ \dfrac{1}{L_o} \end{bmatrix} V_{PN} \tag{15}$$

Eqs. (5), (14) and (15) are the key factors for the proposed mathematical and control models.

B. Design of the Slide Mode Controller

According to the analysis above, the principle diagram of the slide mode controller operational principle is shown in Fig. 7. The working process is as follows: the sensor detects the DC output voltage V_o that will be compared with the desired output voltage V_{ref}. This determines the error value. Then, the error value is sent to the RL-SMC controller based on the reaching law. Then, the modulation index m will be calculated. The sensor detects the phases of the input voltages and currents at the grid side. This determines φ_s, the power factor at the grid side. The phase difference φ_s is sent to the PF SMC controller. Then the phase difference φ_i is determined, and the compensation angle is calculated.

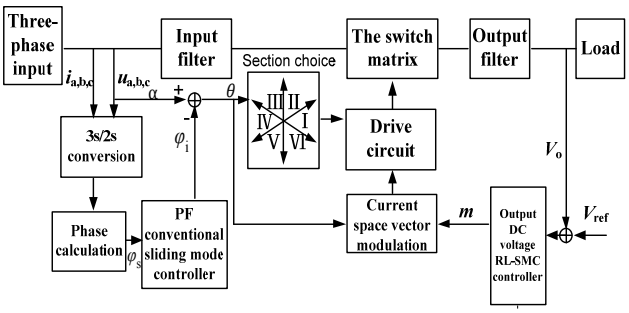

Fig. 7. The principle diagram.

B. DC Output Voltage Regulation by the RL-SMC

The control system is designed to suppress the DC output voltage fluctuations caused by an unbalanced input three-phase voltage. The controller allows the DC output voltage V_o track the reference voltage V_{ref}.

$$e_v = V_{ref} - V_o \tag{16}$$

Where e_v is the feedback voltage error value. In addition, $\dot{e}_v = -\dot{V}_o$. Thus, Eq.(16) is shown as:

$$\begin{bmatrix} \dot{e}_v \\ \dot{I}_{dc} \end{bmatrix} = \begin{bmatrix} -\dfrac{1}{R_L C_o} & -\dfrac{1}{C_o} \\ \dfrac{1}{L_o} & 0 \end{bmatrix} \begin{bmatrix} e_v \\ I_{dc} \end{bmatrix} + \begin{bmatrix} \dfrac{1}{R_L C_o} \\ -\dfrac{1}{L_o} \end{bmatrix} V_{ref} + \begin{bmatrix} 0 \\ \dfrac{1}{L_o} \end{bmatrix} V_{PN} \tag{17}$$

The slide mode function is shown as:

$$S_1 = e_v + c_1 \dot{e}_v \tag{18}$$

where c_1 is a positive constant.

$$\dot{S}_1 = \dot{e}_v + c_1 \ddot{e}_v = \left(-1 + \frac{c_1}{R_L C_O}\right)\dot{e}_v - \frac{c_1}{R_L C_O}(V_{PN} - V_O) \tag{19}$$

In Eq. (19), when $c_1 \approx R_L C_O$, $\left(-1 + \dfrac{c_1}{R_L C_O}\right) \approx 0$ or $c_1 < R_L C_O$, $\left|-\dfrac{c_1}{R_L C_O}(V_{PN} - V_O)\right| \gg \left|\left(-1 + \dfrac{c_1}{R_L C_O}\right)\dot{e}_v\right|$. Thus, Eq. (19) can be simplified as:

$$\dot{S}_1 = -\frac{c_1}{L_o C_o}(V_{PN} - V_o) \tag{20}$$

In order to achieve a higher dynamic performance of the DC output voltage, the exponent reaching law is applied:

$$\dot{S}_1 = -\varepsilon_1 \mathrm{sgn} S_1 - k S_1 \tag{21}$$

Where ε_1 and k are positive constants. From Eq. (20) and

Eq. (21), it can be know that:

$$-\frac{c_1}{L_oC_o}(V_{PN}-V_o)=-\varepsilon_1\mathrm{sgn}S_1-kS_1 \tag{22}$$

From Eq. (5) and Eq. (22), the modulation index m can be shown as:

$$m=\begin{cases}\dfrac{V_o}{1.5V_{im}\cos\varphi_i}+\dfrac{L_oC_o}{1.5c_1V_{im}\cos\varphi_i}(\varepsilon_1+kS_1) & S_1>0\\ \dfrac{V_o}{1.5V_{im}\cos\varphi_i}-\dfrac{L_oC_o}{1.5c_1V_{im}\cos\varphi_i}(\varepsilon_1+k|S_1|) & S_1<0\end{cases} \tag{23}$$

C. Grid Side Power Factor Compensated by the Constant Reaching Law

The control system is also designed to compensate the power factor at the grid side. This control algorithm is able to compensate the phase of the input current at the grid side by applying the SMC. Thus, it can guarantee that the phase φ_s is zero in theory. The switching function is set as:

$$S_2=\varphi_s+c_2\dot{\varphi}_s \tag{24}$$

Where, $\dot{\varphi}_s$ is the average rate of change. Meanwhile the control function is as follows:

$$\varphi_i=\begin{cases}\varphi_{ref}-\delta=\dfrac{3\omega R_LC_iU_{sm}^{\ 2}}{V_{ref}^{\ 2}}-\delta & S_2<0\\ \varphi_{ref}+\delta=\dfrac{3\omega R_LC_iU_{sm}^{\ 2}}{V_{ref}^{\ 2}}+\delta & S_2>0\end{cases} \tag{25}$$

where, φ_{ref} is the pre-compensation angle. The phase δ is the disturbance resist factor and $|\varphi_i|\le\pi/6$. To achieve the local reachability of theSMC, Eq. (25) should be satisfied as:

$$S_2\dot{S}_2<0 \tag{26}$$

where $\dot{S}_2$ is the time derivative of S_2.

$$S_2\dot{S}_2=(\varphi_s+c_2\dot{\varphi}_s)\dot{S}_2 \tag{27}$$

If c_2 is small enough, $S_2=\varphi_s$ and Eq. (27) can be simplified as follows:

$$S_2\dot{S}_2=\varphi_s\dot{S}_2=\varphi_s(\dot{\varphi}_s+c_2\ddot{\varphi}_s) \tag{28}$$

From Eq. （13）, $\dot{\varphi}_s=\dot{\varphi}_i$ and $\ddot{\varphi}_s=\ddot{\varphi}_i$. Because φ_s and φ_i are nonlinear functions, $\dot{\varphi}_s$ and $\dot{\varphi}_i$ are the change rates of φ_s and φ_i in the control cycle. As a result, $\ddot{\varphi}_s$ and $\ddot{\varphi}_i$ are also the change rates of $\dot{\varphi}_s$ and $\dot{\varphi}_i$.

1） If $S_2>0$, then $\varphi_s>0$.

From Eq. (25), in the next control cycle, there is $\varphi_i=\varphi_{ref}-\delta$. Meanwhile $\dot{\varphi}_i=(-\delta-\delta)f_s=-2\times10^4\delta$ and $\ddot{\varphi}_i=(-2\delta f_s-2\delta f_s)f_s=-4\times10^8\delta$, where f_s is the switching frequency and $f_s=10^4$. Substituting the above-mentioned expressions of $\dot{\varphi}_i$ and $\ddot{\varphi}_i$ into the Eq. (28), inequality (26) holds, which means that the sliding mode exists [20].

2） If $S_2<0$, then $\varphi_s<0$.

From Eq. (25), in the next control cycle, there is $\varphi_i=\varphi_{ref}+\delta$. Meanwhile $\dot{\varphi}_i=(\delta+\delta)f_s=2\times10^4\delta$ and $\ddot{\varphi}_i=(2\delta f_s+2\delta f_s)f_s=4\times10^8\delta$. Substituting $\dot{\varphi}_i$ and $\ddot{\varphi}_i$ into Eq. (28), inequality (26) also holds, which means that the sliding mode exists.

The value range discussion of the sliding mode coefficient: if c_2 is small enough to make the equality $S_2=\varphi_s+c_2\dot{\varphi}_s\approx\varphi_s$ and $|\dot{\varphi}_s|=|\dot{\varphi}_i|=|-2\times10^4\delta|$, then $c_2\dot{\varphi}_s<\frac{1}{10}\varphi_s$ when $c_2<\frac{\varphi_s}{10}\times\frac{1}{2\times10^4\delta}$, consequently:

$$c_2<\frac{\varphi_s}{2\delta}10^{-5} \tag{29}$$

From Eq. (29), the value of the sliding mode coefficient is related to the switching frequency and the control function (25).

TABLE I
PARAMETERS OF THE SIMULATION

source voltage	50 V
source frequency	50 Hz
inductance of input filter L_i	2 mH
capacitor of input filter C_i	20 μF
damping resistance of input filter R_i	15 Ω
inductance of output filter L_o	5 mH
capacitor of output filter C_o	20 μF
Load resistance R_L	30 Ω
sliding mode coefficient c_1 , c_2	2×10^{-5} ,1×10^{-5}
ε_1	100
k	200

IV. SIMULATION AND EXPERIMENTAL RESULTS

In this section, a detailed simulation is built on the MATLAB/SIMULINK platform to verify the proposed control strategy.

A. Simulation and its Analysis

The circuit parameters listed in Table I are used in the small-scale simulation model. Three comparative simulations were carried out in this section: (1) balance input with different values of c_1; (2) three-phase balanced input voltage using the conventional SMC; (3) three-phase balanced input voltage using the SMC based on the reaching law; and (4) three-phase unbalanced input voltage using the SMC based on the reaching law. The simulation waveforms and the results of the total harmonic distortions are shown in Fig. 9 to Fig. 11.

Fig. 8 shows a simulation with different values of c_1 under the balance input condition. In simulation (a) $c_1=6\times10^{-4}=R_LC_O$ and in simulation (b) $c_1=2\times10^{-6}<R_LC_O$. From the simulations results it can be seen that the former

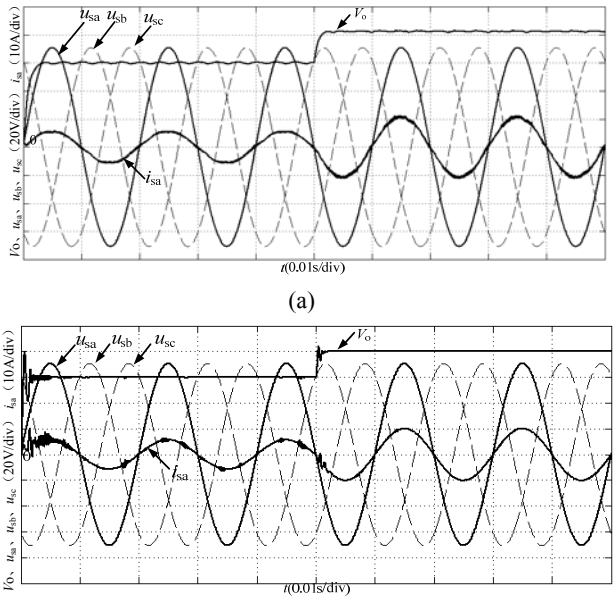

Fig. 8. Experimental results when the input is balanced but with different value of c_1: (a) c_1=6×10^{-4}; (b)c_1=2×10^{-6}.

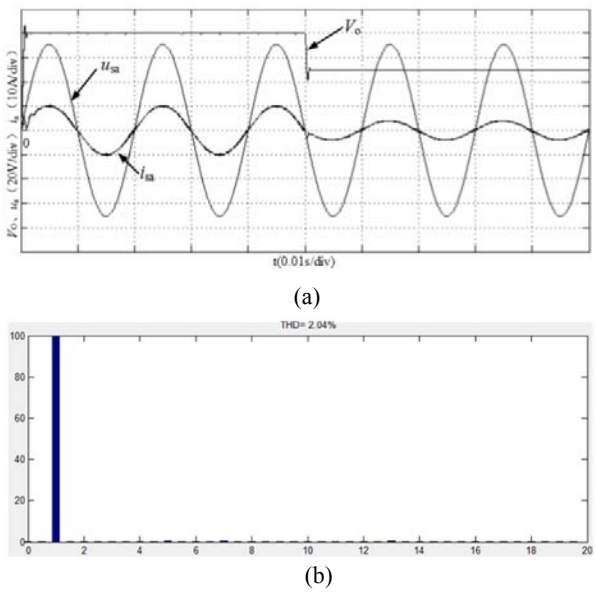

Fig. 9. Experimental results of using conventional SMC when the input voltage is balanced: (a) simulation waveform; (b) THD analysis.

DC output performance is worse than latter since a larger value of c_1 makes the $c_1\dot{e}_v$ part become larger and deteriorates the control precision.

A comparative simulation study was conducted using the same circuit parameters but with different control strategies. Both the conventional SMC and the SMC based on the reaching law were used. According to Fig. 9 and Fig. 10, using the two above-mentioned approached can achieve two goals, ripple-free output voltage and a near unity power factor. Moreover the chattering of the waveform is acceptable. At 50 ms, the target output voltage dropped from 80 V to 50 V. The

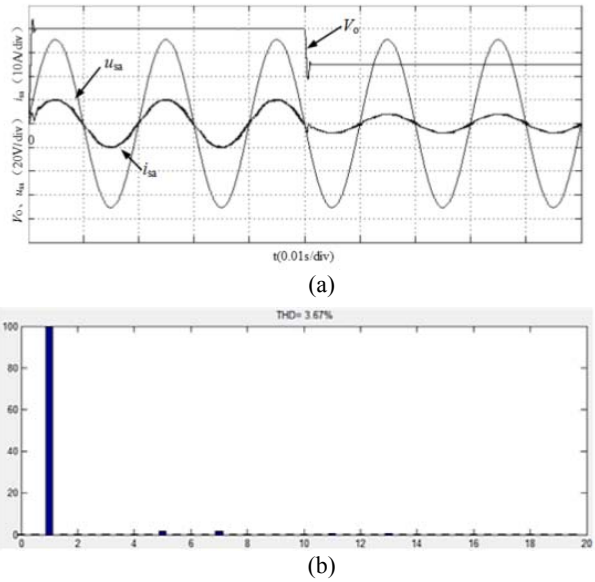

Fig. 10. Experimental results of using SMC based on reaching law when the input voltage is balanced: (a) simulation waveform; (b) THD analysis.

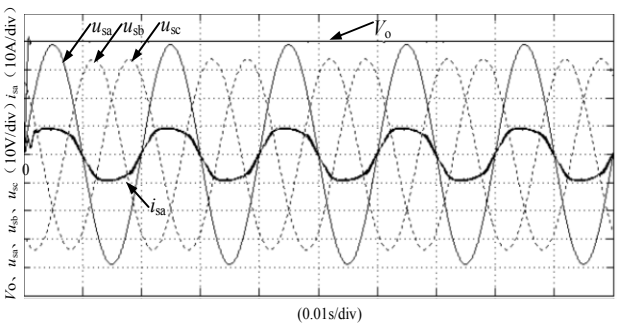

Fig. 11. Simulation waveform using SMC based on reaching law when the input voltage is unbalanced.

simulation results proved that the dynamic performance was excellent regardless of which control algorithm was used.

According to Fig. 11, when the three-phase input voltage is unbalanced, applying the RL-SMC algorithms on the MR can provide a ripple-free output voltage.

B. Experimental Results and their Analysis

An experimental prototype was built to further illustrate and validate the proposed control approach. Three comparative experiments were carried out: (1) a three-phase balanced input voltage using the conventional SMC; (2) a three-phase balanced input voltage using the SMC based on the reaching law; and (3) a three-phase unbalanced input voltage using the SVM algorithm without any compensation and using the SVM algorithm compensated by the SMC based on the reaching law, respectively.

From Fig. 12(a), using the conventional SMC algorithm can achieve both output voltage regulation and a higher power factor. However, it also has a drawback since it can only be

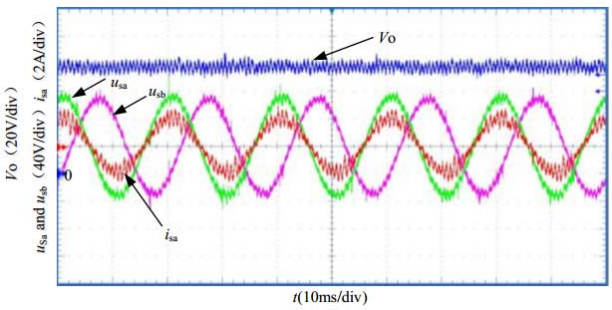

(a)

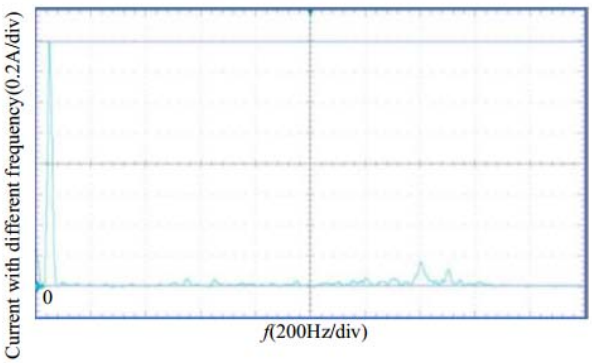

(b)

Fig. 12. Experimental results of using conventional SMC compensation algorithm:(a) AC supply at the grid side and the DC output voltage; (b) spectrum analysis of the A-phase input current.

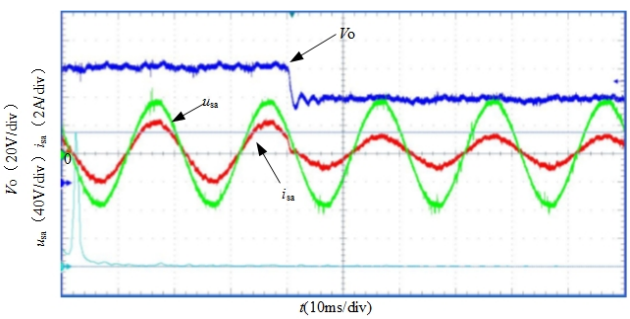

(a)

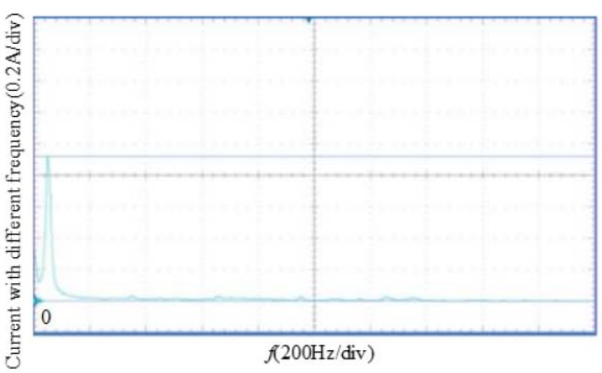

(b)

Fig. 13. Experimental results of using SMC compensation based on the reaching law when the three-phase input supply voltage is balanced:(a) AC supply at the grid side and the DC output voltage; (b) spectrum analysis of the A-phase input current.

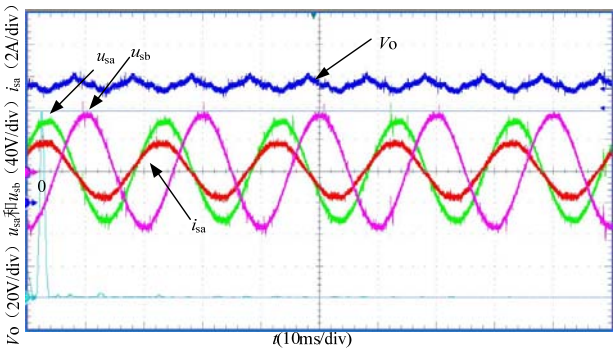

(a)

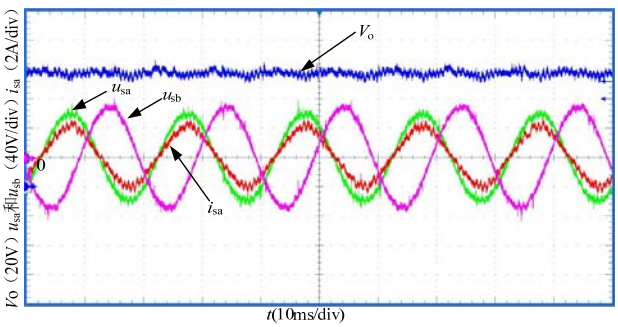

(b)

Fig. 14. Experimental results when the AC voltage supply is unbalanced: (a) using the SVM algorithm; (b) using the RL-SMC algorithm.

switch to two modes and cannot change the states according to the running condition. In the dynamic process it requires the system mode switch in a wide range, but for the steady state operation this kind of wide range switch is not conducive to the output performance. As shown in Fig. 12(b), the frequency of the current harmonic is mainly located near 1.4kHz. Using the same circuit parameters, but applying the reaching law can solve this problem effectively through changing the switch state to adapt to different working condition. The experimental waveform applying the RL-SMC are as shown in Fig. 13(a) and Fig. 13(b). In addition, Fig. 13 (a) shows the target voltage undergo a mutation from 80V to 60V, with a response time of 4ms.

According to Fig. 14(a), using the SVM algorithm without any compensation control approach, to control the MR results in a ripple in the output voltage and a decrease in the power factor at the grid side in the case of unbalanced sinusoidal supply voltages. However, under the same conditions, using the SVM algorithm with compensation by the RL-SMC based on the reaching law and NSMC can effectively achieve both output voltage regulation and power factor control, as shown in the Fig. 13(b). The experimental results show good agreement with the theoretical analysis.

However, the RL-SMC algorithm proposed in this paper cannot alleviate chattering well, and the simulation results

and experiment results are not the same, due to non-ideal bidirectional switches operating in the real experiment instead of the simulation environment.

V. Conclusion

The novel approach of achieving both a tight DC voltage regulation and direct power factor control by the SVM compensated by the SMC based on the reaching law has been theoretically justified and experimentally verified. A simple single-phase model of a three-phase ac-DC matrix rectifier has been proposed. Its effectiveness has been verified through simulation and experimental results.

The experimental results also demonstrate that applying a sliding mode control based on the reaching law can improve the robustness and dynamic performance of the matrix rectifier. Furthermore, the proposed control method is also capable of wide leading or lagging power factor operation which may broaden its application rang.

References

[1] J. W. Kolar, T. Friedli, J. Rodriguez, and P. W. Wheeler, "Review of three-phase PWM AC–AC converter topologies," *IEEE Trans. Ind. Electron.*, Vol. 58, No. 11, pp. 4988-5006, Nov. 2011.

[2] P. W. Wheeler, J. Rodriguez, J. C. Clare, L. Empringham, and A. Weinstein, "Matrix converter: a technology review," *IEEE Trans. Ind. Electron.*, Vol. 49, No. 2, pp. 276-288, Apr. 2002.

[3] D. G. Holmes and T. A. Lipo, "Implementation of a controlled rectifier using AC-AC matrix converter theory," *IEEE Trans. Power Electron.,* Vol. 7, No. 1, pp. 240-250, Jan. 1992.

[4] Z. Xu, G. X. Yin, and D. G. Xu, "A new bidirectional AC–DC converter using a matrix converter topology," *Transactions of China Electrotechnical Society*, Vol. 26, No. 8, pp.64-70, Aug. 2011.

[5] M. Venturini and A. Alesina, "The generalized transformer: a new bidirectional sinusoidal waveform frequency converter with continuously adjustable input power factor," in *IEEE Power Electronics Specialists Conference (PESC)*, pp. 242-252. 1980.

[6] G. Roy and G. E. April, "Cycloconverter operation under a new scalar control algorithm," in *20th Annual IEEE Power Electronics Specialists Conference (PESC)*, Vol. 1, pp. 368-375, Jun. 1989.

[7] D. Casadei, G. Serra, A. Tani, and L. Zarri, "Matrix converter modulation strategies: a new general approach based on space-vector representation of the switch state," *IEEE Trans. Ind. Electron.*, Vol. 49, No. 2, pp. 370-381, Apr. 2002.

[8] X. Y. Liu, B. Zhou, H. Q. Xian, and M. M. Shi, "Investigation on grid side power factor of two stage matrix converter," *Transactions of China Electrotechnical Society*, Vol. 27, No.12, pp. 71-78, Dec. 2012.

[9] W. Cai, X. J. Yang, and Y. M. Gong, "Research on power characteristics of matrix rectifier," *Automation of Electric Power Systems*, Vol. 30, No. 8, pp. 27-31, Aug. 2006.

[10] Z. P. Wang, Y. X. Xie, K. Yang, and M. Luo, "Feedforward fuzzy compensation control of matrix rectifier in abnormal conditions," *Electric Power Automation Equipment*, Vol. 34, No. 5, pp. 98-104, May 2014.

[11] X. N. Lu, K. Sun, and G. Li, "Control method analysis of grid side power factor in two stage matrix converter," *Transactions of China Electrotechnical Society*, Vol. 25, No. 10, pp. 108-114, Oct. 2010.

[12] J. D. Zhu, Z. Xu, B. H. Jiang, and C. H. Zhang, "Close-loop control of an AC-DC matrix converter for automotives," in *IEEE Electrical Power and Energy Conference (EPEC),* pp. 426-431, Oct. 2011.

[13] W. L. Deng, X. R. Yang, and J. L. Zhu, "Study of closed loop control based on double synchronous rotating frame for two-stage matrix converter under unbalanced load," *Proceedings of the CSEE*, Vol. 26, No. 10, pp. 70-75, Oct. 2006.

[14] H. M. Nguyen, H.-H. Lee, and T.-W. Chun, "Input power factor compensation algorithms using a new direct-SVM method for matrix converter," *IEEE Trans. Ind. Electron.*, Vol. 58, No. 1 pp. 232-243, Jan. 2011.

[15] X. Liu, Q. F. Zhang, and D. L. Hou, "Sliding mode variable structure control of matrix rectifiers," *Transactions of. China Electrotechnical Society*, Vol. 28 No. 4, pp. 149-164, Apr. 2013.

[16] M. Venturini and A. Alesina, "The generalized transformer: a new bidirectional sinusoidal waveform frequency converter with continuously adjustable input power factor," in *IEEE Power Electronics Specialists Conference (PESC)*, pp. 242–252, 1980.

[17] A. Alesina and M. Venturini, "Intrinsic amplitude limits and optimum design of 9-switches direct PWM AC–AC converters," in *IEEE Power Electronics Specialists Conference(PESC)*, Vol. 2, pp. 1284-1291, Apr. 1988.

[18] M. K. Kiran and A. Srinivasulu, "Matrix converter using svm method with input power factor compensation," *IOSR Journal of Electrical and Electronics Engineering*, Vol. 2, No. 4, pp. 1-10, Oct. 2012.

[19] X. Liu, Q. F. Zhang, D. L. Hou, and S. Y. Wang, "Improved space vector modulation strategy for AC-DC matrix converter," *Journal of Power Electronics*, Vol. 13, No. 4, pp. 647-655, Jul. 2013.

[20] S. C. Tan, Y. M. Lai, and C. K. Tse, "Indirect sliding mode control of power converters via double integral sliding surface," *IEEE Trans. Power Electron.*, Vol. 23, No. 2, pp. 600-611, Mar. 2008.

Zhiping Wang was born in Dongguan, Guangdong Province, China, in 1978. He received his B.S. and M.S. degrees from the South China University of Technology (SCUT), Guangzhou, China. He is presently working towards his Ph.D. degree in Electrical Engineering in the School of Electrical Power, South China University of Technology. He is presently working as an Associate Professor at the Guangdong Institute of Automation, Guangzhou, China. His current research interests include high-power density rectifiers and control strategies.

Yunshou Mao was born in Guangzhou, Guangdong Province, China, in 1989. He received his B.S. degree in Electronics and Engineering from the North University of China (NUC), Taiyuan, China, in 2013. He is presently working towards his M.S. degree in Electrical Engineering at the Guangdong University of Technology (GDUT), Guangzhou, China. His current research interests include high-power density rectifiers, multilevel converters and control strategies.

Zhanhu Hu was born in Zhanjiang, Guangdong Province, China, in 1965. He received his B.S., M.S., and Ph.D. degrees in Computer Information Systems Engineering and in Computer Application and Aerospace Control Engineering from the Northwestern Polytechnical University, Xi'an, China, in 1988, 1991, and 1999, respectively. He was a postdoctoral researcher from 1999 to 2001 in Nanjing. He is presently working as a Professor at the Guangdong Institute of Automation, Guangzhou, China. His current research interests include wavelet theory, control engineering and signal processing.

Yunxiang Xie was born in Shaoyang, Hunan Province, China, in 1965. He received his B.S., M.S., and Ph.D. degrees in Electrical Engineering from Xian Jiaotong University, Xian, China, in 1985, 1988, and 1991, respectively. He was a postdoctoral researcher from 1991 to 1994. He was an Associate Professor from 1994 to 1999, and has been a Professor since 1999, in the School of Electrical Power, South China University of Technology, Guangzhou, China. His current research interests include power electronics and control, including high-power density rectifiers, multilevel converters, active filters, and distributed power quality and control strategies.